

## Robust Correction of 3D Error Fields in Tokamaks including ITER

J.-K. Park<sup>1</sup>, J. E. Menard<sup>1</sup>, M. J. Schaffer<sup>2</sup>, H. Reimerdes<sup>3</sup>, A. H. Boozer<sup>3</sup>, R. J. Buttery<sup>2</sup>, C. M. Greenfield<sup>2</sup>, D. A. Gates<sup>1</sup>, S. P. Gerhardt<sup>1</sup>, R. J. La Haye<sup>2</sup>, R. M. Nazikan<sup>1</sup>, S. A. Sabbagh<sup>2</sup>, J. A. Snipes<sup>4</sup>, J. T. Scoville<sup>2</sup>, S. M. Wolfe<sup>5</sup>, the NSTX Research Team, the DIII-D Research Team, and the TBM International Research team

<sup>1</sup>Princeton Plasma Physics Laboratory, Princeton, New Jersey, USA

<sup>2</sup>General Atomics, San Diego, California, USA

<sup>3</sup>Columbia University, New York, New York, USA

<sup>4</sup>ITER Organization, Route de Vinon sur Verdon, 13115 Saint Paul Lez Durance, France

<sup>5</sup>MIT Plasma Science and Fusion Center, Cambridge, Massachusetts, USA

E-mail contact of main author: [jpark@pppl.gov](mailto:jpark@pppl.gov)

**Abstract.** Important progress has been made in the correction of 3D fields, based on the improved understanding of plasma response using the Ideal Perturbed Equilibrium Code (IPEC). The key to error field correction is to reduce the dominant distribution of 3D fields that is stronger often by an order of magnitude than any other distribution in breaking magnetic surfaces. The important validation is achieved in presently the most extreme case, the DIII-D mock-up experiments for the ITER Test Blanket Modules (TBMs). Although the TBM 3D fields are highly localized and cannot be controlled by typical error field correction coils, the optimal operation could be restored using I-coils by minimizing the dominant part in the TBM 3D fields as IPEC prediction. Including TBM experiments, various error field correction results in tokamaks such as NSTX, DIII-D, and CMOD, have been successfully understood and quantified based on the dominant external fields, as can be summarized in the robust parametric scaling of the locking threshold. The implications are favourable for ITER, since the highly reliable 3D field compensation can be provided for a wide range of different plasmas if the correction coil is designed based on the robust patterns of the dominant external fields. Present Error Field Correction Coil (EFCC) in ITER is under active investigations using IPEC to assess their capabilities.

### 1. Introduction

The correction of 3D fields is important to improve tokamak performance. The 3D fields can destroy and deform magnetic surfaces, and subsequently induce plasma locking [1-4] or unnecessary rotational damping by Neoclassical Toroidal Viscosity (NTV) [5-8]. The theoretical understanding of plasma response to 3D fields has been recently improved using the Ideal Perturbed Equilibrium Code (IPEC) [9-12] and also using the ideal version of MARS-F [13]. The core result is that the field driving magnetic islands and plasma locking is not the external (vacuum) resonant fields, but the total resonant fields including ideal plasma response. In the past, external resonant fields have been used as an approximation for the total resonant fields, but their differences can be unexpectedly large in actual tokamaks.

The total resonant fields are the good measures for plasma locking, but it is still required to understand how the external 3D fields couple to the total resonant fields for the effective control of 3D fields. A useful quantity is the *dominant external field*, which is defined at the plasma boundary surface and represents the external field dominantly producing the total resonant fields at the rational surfaces. One can assume that the dominant external field is the unique distribution to produce the total resonant fields as a good approximation since other external field distributions are less important often by an order of magnitude than the dominant external field [11]. The approximation can greatly simplify the control of 3D fields, as far as locking physics is only concerned, since the structure of the dominant external field

is highly robust across different plasmas and configurations. Recent ITER [14] Test Blanket Modules (TBMs) mock-up experiments [15] in DIII-D [16] provided a very good example of the importance of the dominant external field in 3D error field corrections, with an extreme difference between TBM 3D fields and correction coil fields. The results are consistent with other error field correction results, and thus can be combined into global parametric scaling to predict and design error field corrections in other tokamaks including ITER [17].

## 2. The correction of TBM 3D fields

The TBM 3D fields are highly localized and cannot be controlled by typical error field correction coils, such as C-coils or I-coils in DIII-D. Their external field spectra are shown in Figure 1 (a) and (b), and one can see that the TBM 3D fields are the sum of many different toroidal and poloidal harmonic perturbations. There is the minimum in the spectral amplitudes as seen in Figure 1 (b), which in fact almost null the ( $m=2/n=1$ ) external resonant field. However, the  $n=1$  total resonant fields calculated from IPEC, as shown in Figure 1 (c), are comparable to the total resonant fields by DIII-D intrinsic errors, and thus considerable plasma locking is expected with TBM 3D fields similarly to intrinsic error fields.

The standard technique in locking experiments [18] is used to investigate the effects of TBM 3D fields on locking and the results are compared with IPEC predictions. Figure 2 shows the time traces of plasma currents, density, I-coil currents to cancel the intrinsic error fields, TBM currents, and magnetic measurements to detect locked modes. One can see that TBM 3D fields produced locked modes in higher density (Red) compared to the case without TBM 3D fields (Black). The observed locking could be induced directly by resonant components as IPEC predictions, but also might be resulted from the effects of all other non-resonant components that can reduce plasma rotations and thus make plasmas more vulnerable to the existing intrinsic error fields.

In order to separate these two possibilities, the  $n=1$  error field corrections are applied using I-coils. If the plasma locking is caused indirectly by non-resonant components, then the corrections for the  $n=1$  resonant components would not be successful. I-coil currents and

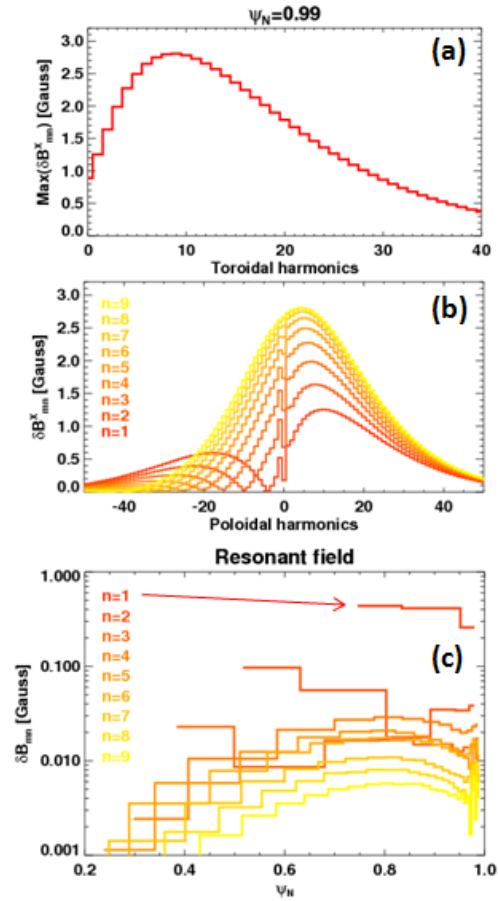


FIG 1. Field spectra of TBM 3D fields. The (a) shows maximum poloidal harmonic amplitudes vs. toroidal harmonics, and (b) shows poloidal spectra for  $n=1\sim 9$  toroidal harmonics, for the external field on the plasma boundary surface (calculated by SURFMN [19]). (c) is the total resonant fields for  $n=1\sim 9$  toroidal harmonics (calculated by IPEC).

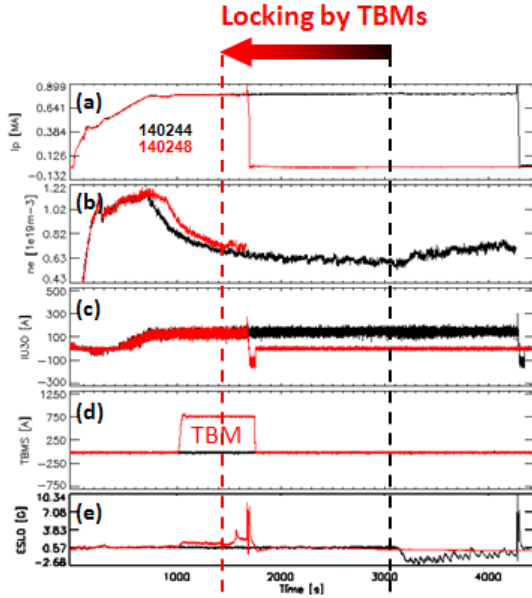


FIG 2. TBM effects on plasma locking : Time traces for (a) plasma currents, (b) density, (c) I-coil currents, (d) TBM currents, (e)  $B_p$  sensor diagnostics for shots with (Red) and without (Black) TBMs. One can see TBM induced locking at higher density.

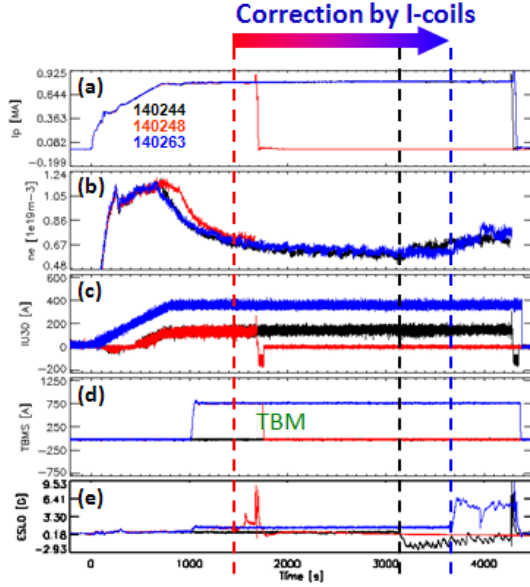


FIG 3. I-coil  $n=1$  correction (Blue) mitigated locking and restored the locking density as low as the case without TBMs (Black) from the high locking density with TBMs (Red). Time traces are same as Figure 2.

toroidal phases were optimized using the standard techniques [18] and the optimized corrections were applied to compensate TBM 3D fields. The corrections indeed recovered the locking density as low as the case without TBM error fields, as one can clearly see from Figure 3. The IPEC analysis for these experiments verifies that the 2/1 total resonant field is the most critical parameter for TBM 3D fields to avoid locking, as seen by the good correlation with plasma density. This is expected from ideal plasma response calculations, but it is still striking that the two very different 3D fields, TBM 3D fields and I-coil 3D fields can compensate each other and can result in the mitigation of plasma locking as observed.

### 3. The dominant external field driving plasma locking

An intuitive understanding of the TBM error field correction results can be obtained by considering the coupling between the external fields and the total resonant fields. The external fields can be decomposed based on their importance in producing the total resonant fields. One can use SVD techniques for the coupling matrix between the external fields on the plasma boundary and the total resonant fields, and can obtain the most important external field in driving the total resonant fields. The resulting distribution of the external fields is defined as the *dominant external field*, since other orthogonal distributions are less important often by an order of magnitude. The 3D shape of the dominant external field can be expressed by  $\delta \vec{B}_{dcn}^x \cdot \hat{n}_b = C(\theta) \cos n\varphi + S(\theta) \sin n\varphi$ , where  $C(\theta)$  and  $S(\theta)$  are the Cosine and Sine field distributions, and the subscript *dcn* indicates the dominant external field for the core for each  $n$  toroidal harmonic perturbation [11].

Figure 4 shows the (a) Cosine and (b) Sine field distributions of the dominant external field (Red) relative to the plasma boundary (Black), for a target plasma used in TBM error field correction experiments. The error fields including intrinsic machine errors and TBM 3D fields are also shown (Green). One can easily find TBM 3D fields as marked in Figure 4 (b). The  $n=1$  TBM 3D fields are relatively broader in shape compared to their higher  $n$  components, but are still highly localized and thus cannot be controlled by I-coil correction fields. However, I-coil correction fields can be coupled well to the dominant external field. It implies that I-coils can control plasma locking since one can assume that the dominant external field is the almost only distribution that drives plasma locking. One can see the corrected shape of 3D fields (Blue) has the unchanged TBM 3D fields as the uncorrected shape (Green), but Sine distribution is modified by I-coils as can be seen from the difference between the corrected shape (Blue) and the uncorrected shape (Green) in Figure 4 (b). The resulting distribution (Blue) has less coupling to the dominant external field (Red) compared to the uncorrected distribution (Green), and thus can mitigate locking as observed.

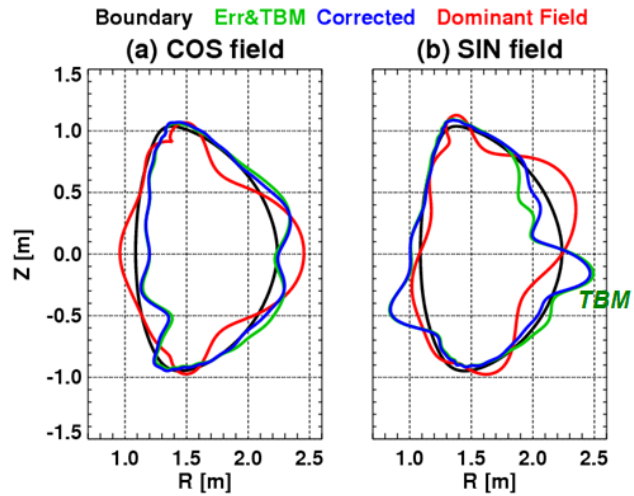


FIG 4. The Cosine and Sine distributions of 3D fields, total errors including intrinsic errors and TBMs (Green), I-coil correction + total errors (Blue), and dominant external field (Red), relative to the plasma boundary (Black). TBM 3D fields can be seen in Sine distributions.

The results imply that the correction coils can be efficiently designed by considering only the coupling to the shape of the dominant external field, even without knowledge of intrinsic error fields in details. The importance of the dominant external field is demonstrated even in an extreme case such as TBM errors as shown, but also can be seen in empirical corrections of 3D error fields in many US tokamaks. Note that the dominant external field is distributed mainly nearby the outboard midplane, and this feature is very robust across plasmas and configurations [11]. The effects of OH-TF joint errors in NSTX [19-20] on locking can be effectively mitigated by a correction field from the outboard side with the only ~5% field amplitude of the

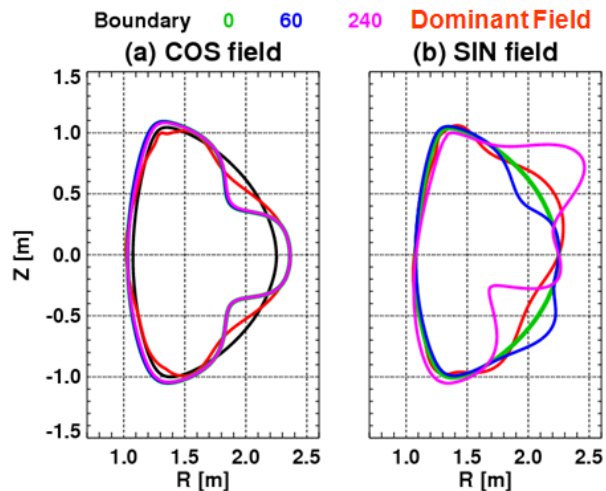


FIG 5. The Cosine and Sine distributions of I-coil fields with different toroidal phasing between the upper and the lower row of I-coils,  $0^\circ$  (Green),  $60^\circ$  (Blue),  $240^\circ$  (Magenta), compared to dominant external field (Red).

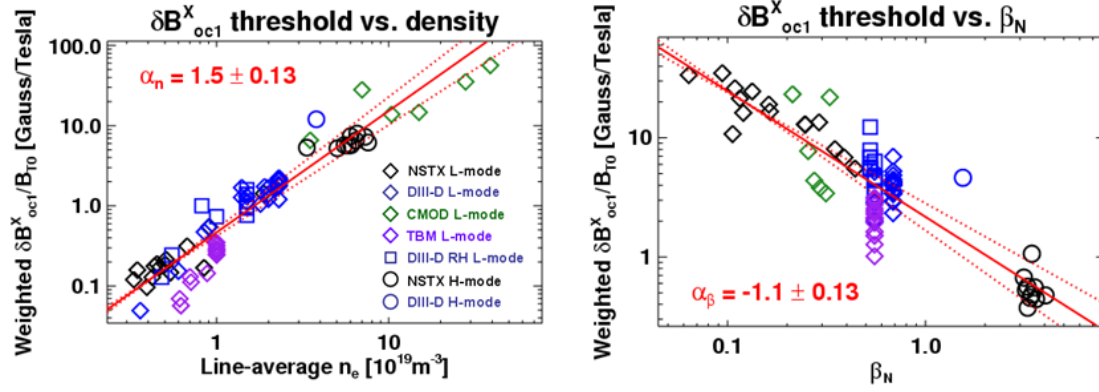


FIG 6. The locking scaling using the  $n=1$  overlap external field. The scaling includes NSTX, DIII-D, and CMOD data for L-mode and/or H-mode, and also TBM cases. The (a) shows the correlation with plasma density and (b) shows the correlation with the normalized plasma  $\beta$ .

intrinsic error fields at the inboard side, since the field can be coupled much better at the outboard side than the inboard side. DIII-D I-coil corrections are known to be optimal with  $240^\circ\sim 300^\circ$  toroidal phasing between upper and lower set of I-coils, since then I-coil fields become similar to the dominant external field, as illustrated in Figure 5. Note that all three different phasing gives the same Cosine distribution with very weak coupling to the dominant Cosine distribution, but the  $240^\circ$  toroidal phasing gives the strongest coupling to the dominant Sine distribution. If  $B_T$  is reversed, the optimal phasing becomes  $\sim 120^\circ$  ( $-240^\circ$ ) as validated in experiments [18] since the helical twist of the dominant external field will also be reversed. Also, CMOD [21] A-coil correction can be effective despite the large distance to the plasmas since the coils can control the fields at the outboard side.

#### 4. The overlap external field and locking scaling

The dominant external field is the almost only distribution to cause plasma locking, and thus precise quantifications for the error field threshold can be obtained if a critical parameter determining the dominant part in a 3D field is used and correlated with plasma parameters. The so-called *overlap external field*,  $\delta B_{ocn}^x$ , is defined as

$$\delta B_{ocn}^x = \int d\varphi' \int da \frac{(\delta \vec{B}^x \cdot \hat{n}_b)(\mathcal{G}, \varphi' - \varphi)(\delta \vec{B}_{dcn}^x \cdot \hat{n}_b)(\mathcal{G}, \varphi)}{|\delta \vec{B}_{dcn}^x \cdot \hat{n}_b(\mathcal{G}, \varphi)|},$$

where  $da$  indicates that the surface integration on the boundary is required. Using the overlap external field, various locking data in tokamaks have been investigated, as illustrated in Figure 6. The resulting  $n=1$  field threshold is given by

$$\delta B_{ocn}^x / B_{T0} \leq 0.4 \times 10^{-4} (n[10^{19} m^{-3}])^{1.5} (B_{T0}[T])^{-1.9} (R_0[m])^{1.2} \beta_N^{-1.1}.$$

The scaling has been obtained across 3 US tokamaks, NSTX, DIII-D, CMOD, and includes TBM, Ohmic, H-mode, and reversed  $B_T$  (Right-Handed, RH) experiments, but the standard deviation is mostly less than only  $\sim 10\%$  except the size scaling that has  $\sim 20\%$ . Note the threshold is almost proportional to the inverse  $\beta_N$ , indicating that the sensitivity of tokamak plasmas to 3D fields becomes greater in higher  $\beta_N$  due to the stronger plasma response. In the error field threshold study in H-mode, which has been recently performed in NSTX and DIII-

D [22], the plasma rotation can become another critical parameter since it is not self-determined due to the external drives of the toroidal torque. More thorough investigations for the role of the plasma rotation remain for the future work. In addition, error field correction results in larger tokamaks, such as JET, are desired to improve the size scaling of present data and the reliability for the extrapolation to ITER.

The ITER error field study has been revisited by the new method based on the dominant external field and the

overlap external field [17]. IPEC analysis indicates the midplane Error Field Correction Coil (EFCC) is much more effective than the top and bottom EFCC, but even the midplane EFCC can be less effective depending on ITER scenarios. Figure 7 shows the coupling between the midplane EFCC and dominant 3D fields in various scenarios. The overlap external field in EFCC fields decreases as 12G, 8G, and 7 G, for the two inductive scenarios and the one advance scenario, respectively, indicating proportionally the efficiency to control dominant external field in each scenario. Note that this assessment for ITER EFCC capability is independent on intrinsic error fields since the intrinsic errors also can drive locking only through the dominant external fields.

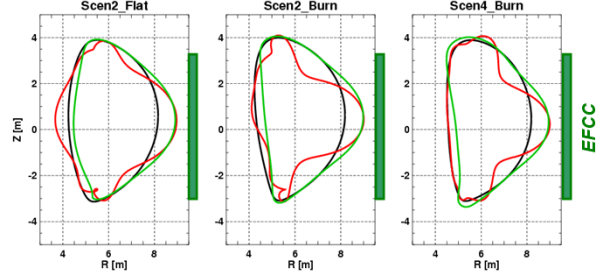


FIG 7. The spatial structure of the midplane EFCC fields (Green) and the Cosine part of the dominant external fields (Red) at the plasma boundary (Black), for different ITER scenarios. Scen2 and Scen4 indicate inductive and advanced scenario, and Flat and Burn indicate the initial flat-top and fully burning stages.

## 5. The overlap and optimization of 3D error field correction

The overlap external fields represent the strength of external fields in driving locking, but do not represent other physics components such as Neoclassical Toroidal Viscosity (NTV) [5-8]. The NTV transport has quadratic dependency on 3D fields, in a complicated manner for each component of 3D fields. Therefore, even though the elimination of the overlap external fields implies no drive for locking, remaining components can drive stronger NTV if the elimination increases other components that are important for NTV transport. In principle, one can perform a new decomposition of the external field distributions for NTV transport, and can find the most important field distribution for NTV, which can be used in optimization of 3D fields to mitigate both locking and NTV [23]. It remains as future work due to its complexity, but one can alternatively and approximately optimize 3D fields by minimizing the norm of the field distributions while maximizing the overlap external fields. The so-called *overlap* is defined as

$$C = \int d\varphi' \int da \frac{(\delta \vec{B}^x \cdot \hat{n}_b)(\mathcal{G}, \varphi' - \varphi)(\delta \vec{B}_{dcn}^x \cdot \hat{n}_b)(\mathcal{G}, \varphi)}{\left| (\delta \vec{B}^x \cdot \hat{n}_b)(\mathcal{G}, \varphi' - \varphi) \right| \left| (\delta \vec{B}_{dcn}^x \cdot \hat{n}_b)(\mathcal{G}, \varphi) \right|}.$$

The overlap measures the percentage of the applied field associated with the dominant external field. The overlap  $C=1$  if the applied field produces only the dominant external field, and  $C=0$  if the applied field produces a distribution that is orthogonal to the dominant external field, that is, if it is entirely irrelevant for locking and thus may worsen other aspects

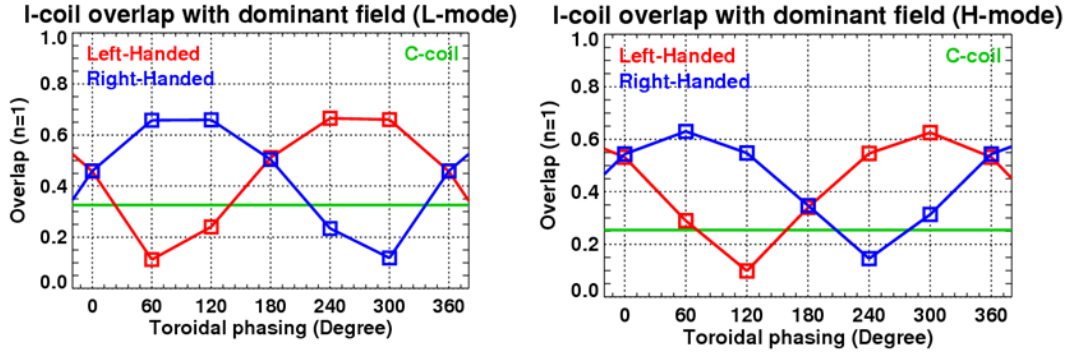


FIG 8. Overlap with dominant external field vs. different toroidal phasing of I-coil configurations for an L-mode and a H-mode case. Overlap for right-handed plasmas are just mirror reflections of the overlap for left-handed plasmas. Note that overlap of C-coil is also shown for comparison.

without any gain for locking. The overlap represents very well the efficiency of correction fields in terms of locking. For example, DIII-D correction coil capabilities can be evaluated based on the overlap, and one can see from Figure 8 that the overlap is highest for the best toroidal phasing ( $240^\circ$  in L-mode and  $300^\circ$  in H-mode as an example) in DIII-D. Also note that C-coil has less efficiency than I-coil best configurations, which is consistent with the empirical observations that C-coil corrections are not as good as I-coil corrections. ITER midplane EFCC is similar to DIII-D C-coils, but the overlap of EFCC  $\sim 25\%$  is typically smaller than the overlap of C-coil  $\sim 33\%$ . This means that it is difficult to expect EFCC coil capability in ITER better than C-coil in DIII-D. However, the overlap is only an approximation to address the remaining components other than the resonant components for locking (dominant external fields), so more thorough analysis for locking and NTV by 3D fields is planned and will be reported for ITER.

## 6. Final Remarks

The 3D error fields can be decomposed by their importance in producing the total resonant fields driving plasma locking. The most important distribution is defined as the dominant external field, which can be assumed as the unique distribution to cause plasma locking since other distributions are less important often by an order of magnitude. Error field correction results for TBM 3D fields demonstrated that one can control plasma locking even if correction coils cannot directly change the imposed 3D fields, as long as correction coils can control the dominant external field. Other typical error field correction results in NSTX, DIII-D, and CMOD, can be consistently understood using the dominant external field. The part of the applied field coupled to the dominant external field is defined as the overlap external field, which can give consistent parametric quantifications for plasma locking across different machines and configurations. Results are favorable to ITER and other next fusion devices, since robust error field corrections can be designed and optimized before the knowledge of intrinsic error fields if one uses the overlap external field and the overlap percentage with the dominant external field. However, better optimization may be required to address other physics issues such as NTV transport.

## Acknowledgment

This work was supported by the US department of Energy under contract DE-AC02-76CH03073 (PPPL), DE-FG02-03ERS496 (CU), and DE-FC02-04ER54698 (GA).

The views and opinions expressed herein do not necessarily reflect those of the ITER Organization.

## References

- [1] Hender, T. C., et al., Nucl. Fusion **32** (1992) 2137
- [2] La Haye, R. J., et al., Phys. Fluids B **4** (1992) 2098
- [3] Scoville, J. T., et al., Nucl. Fusion **43** (2003) 250
- [4] Wolfe, S. M., et al., Phys. Plasmas **12** (2005) 056110
- [5] Linsker, R., et al., Phys. Fluids **25** (1982) 143
- [6] Shaing, K. C., Phys. Plasmas **10** (2003) 1443
- [7] Zhu, W., et al., Phys. Rev. Lett. **96** (2006) 225005
- [8] Park, J.-K., et al., Phys. Rev. Lett. **102** (2009) 065002
- [9] Park, J.-K., et al., Phys. Plasmas **14** (2007) 052110
- [10] Park, J.-K., et al., Phys. Rev. Lett. **99** (2007) 195003
- [11] Park, J.-K., et al., Nucl. Fusion **48** (2008) 045006
- [12] Park, J.-K., et al., Phys. Plasmas, **16** (2009), 056115
- [13] Lanctot, M., et al., Phys. Plasmas **17** (2010), 030701
- [14] Ikeda, K., Nucl. Fusion **47** (2007) S1
- [15] Schaffer, M. J., et al., Proc. 23rd Int. Conf. on Fusion Energy, Korea, IAEA (2008)
- [16] Luxon, J. L., et al., Nucl. Fusion **43** (2003) 1813
- [17] Menard, J. E., et al., "Task on the Study of Error Fields using the Ideal Perturbed Equilibrium Code (IPEC)", ITER Report (2010)
- [18] Park, J.-K., et al., "Error Field Correction in DIII-D Plasmas in Either Handedness", submitted to Nuclear Fusion (2010)
- [19] Ono, M., et al., Nucl. Fusion **40** (2000), 557
- [20] Menard, J. E., et al., Nucl. Fusion **50** (2010) 045008
- [21] Hutchinson, I. H., et al., Phys. Plasmas **1** (1994) 1511
- [22] Buttery, R. J., et al., Proc. 23rd Int. Conf. on Fusion Energy, Korea, IAEA (2008)
- [23] Boozer, A. H., et al., Plasma Phys. Control. Fusion **52** (2010) 104001